1-1-2011

Infrared stimulated luminescence measurements of single grains of K-rich feldspar for isochron dating

Bo Li
University of Hong Kong, bli@uow.edu.au

Sheng-Hua Li
University of Hong Kong

Geoffrey A. T Duller
Aberystwyth University, ggd@aber.ac.uk

Ann G. Wintle
Aberystwyth University, aqw@aber.ac.uk

Infrared stimulated luminescence measurements of single grains of K-rich feldspar for isochron dating

Abstract

This paper explores the use of single grain luminescence measurements in isochron dating of K-rich feldspars. The thermal stability of individual feldspar grains was investigated using pulse annealing methods, which appears to distinguish between K-rich and Na-rich feldspars. A good isochron fit was obtained using synthetic aliquots produced from the single grain data set and the age obtained based on an assumed K content of 13 ± 1% was in good agreement with that obtained using single aliquot measurements (and with other age control).

Keywords

isochron, feldspar, rich, k, grains, single, measurements, luminescence, stimulated, dating, infrared, CAS

Disciplines

Medicine and Health Sciences | Social and Behavioral Sciences

Publication Details

Li, B., Li, S., Duller, G. A. T. & Wintle, A. G. (2011). Infrared stimulated luminescence measurements of single grains of K-rich feldspar for isochron dating. Quaternary Geochronology, 6 (1), 71-81.

Infrared stimulated luminescence measurements of single grains of K-rich feldspar for isochron dating

Bo Li[1], Sheng-Hua Li[1,*], Geoffrey A.T. Duller[2], Ann G. Wintle[2]

1. Department of Earth Sciences, The University of Hong Kong, Pokfulam Road, Hong Kong, China
2. Institute of Geography and Earth Sciences, Aberystwyth University, Aberystwyth SY23 3DB, UK.

Abstract

This paper explores the use of single grain luminescence measurements in isochron dating of K-rich feldspars. The thermal stability of individual feldspar grains was investigated using pulse annealing methods, which appear to distinguish between K-rich and Na-rich feldspars. A good isochron fit was obtained using synthetic aliquots produced from the single grain data set and the age obtained based on an assumed K content of 13±1% was in good agreement with that obtained using single aliquot measurements (and with other age control).

Keywords: K-feldspar, IRSL, single grain, luminescence, recuperation, isochron, dating

1. Introduction

A method of dating has been proposed recently in which the infrared stimulated luminescence (IRSL) of potassium-rich feldspar is measured (Li et al., 2007; 2008a; 2008b), the isochron IRSL (iIRSL) method. In this method, the equivalent doses (D_e) for grains of different diameter were determined using the IRSL signal. Isochrons were constructed by plotting the D_e values as a function of the internal dose rates. The method is similar to the subtraction method proposed by Fleming and Stoneham (1973) for thermoluminescence signals from quartz and feldspar and to more recent isochron methods (e.g. Mejdahl, 1983; Clark, 1994; Zhao and Li, 2002).

Any isochron dating method is critically dependent on the accuracy and precision of the data, and the iIRSL method is no exception. The IRSL measurements were made on aliquots made up

of several thousand grains that had been extracted by heavy liquid separation (selection of grains lighter than 2.58 $g.cm^{-3}$) after sieving to obtain the relevant grain sizes; the age was determined from the slope of the best-fit line. It was assumed that this preparation procedure resulted in potassium-rich grains, enabling the internal dose rate to be estimated using an assumed content of 13±1% (Huntley and Baril, 1997; Zhao and Li, 2005; Li and Li, 2008). The accuracy and precision of the D_e values obtained for a single grain size fraction will depend upon whether the IRSL signals are indeed mainly from KF or from some other feldspars (e.g. sodium-rich feldspar, NaF) that are present.

In the work reported here, single grain measurements have been used to investigate variations in thermal stability and other luminescence characteristics at a smaller observation scale and assess the potential for improving precision in isochron dating by the use of synthetic aliquots. These aspects are investigated by making IRSL measurements on single grains. The presence of NaF grains in the lighter than 2.58 $g.cm^{-3}$ fraction is determined by pulse annealing experiments, as previously used by Tso et al. (1996) to determine the relative thermal stability of KF and NaF. The impact of the presence of NaF grains on the D_e obtained using a multiple-grain aliquot is ascertained by measuring the D_e values for several hundred individual grains. The potential of using single grain measurements and appropriate rejection criteria to isolate KF grains, and therefore improve the precision of D_e determination, is also explored.

2. Samples and experimental procedures

Two sedimentary sand samples from desert areas in Northern China were selected for this study. Sm1 was from below the Holocene soil at the Shimao section in the transition zone between the Mu Us Desert and the Loess Plateau. It was chosen since an optically stimulated luminescence (OSL) age of 9.1±0.5 ka had been obtained on quartz grains from this sample (Li et al., 2008b). The sediment grains were thus considered to be well bleached at deposition. Support for the efficiency of light exposure at deposition was provided by an age of ~200 a being obtained for KF grains from a modern dune in the same area (unpublished data). The iIRSL method had been applied to multiple grain aliquots of the KF fraction for sample Sm1 (Li et al., 2008b). HLD3 was an aeolian sand from the He Er Hong De section in the Hulun Buir Desert

and was selected to provide a second sample upon which to test the pulse annealing procedures. It had a quartz OSL age of 10.8±1.2 ka (Li et al., 2002; Li et al., 2008b).

Heavy liquid separations were carried out at 2.58 and 2.62 g.cm^{-3} on grains from which carbonates and organic material had been removed. The KF fractions (density <2.58 g.cm^{-3}) of different grain sizes (90-125, 125-150, 150-180, 180-212 and 212-250 μm diameter) were used for single grain IRSL measurements which were carried out using a single grain system (Duller et al., 2003) attached to a Risø TL/OSL reader. The KF grains were etched 40 minutes with 10% hydrofluorite acid before IRSL measurements. The KF grains were stimulated using an IR laser (830Δ10 nm, 400 W.cm^{-2}) (Bøtter-Jensen et al., 2003a) and the IRSL signals were detected using a photomultiplier tube with the IRSL passing through a filter pack containing a Schott BG-39 and a Corning 7-59 filter. Single aliquot D_e measurements were made on each grain size of the KF fraction, but using IR emitting diodes (880±80 nm, 150 mW.cm^{-2}) as the stimulation source (Bøtter-Jensen et al., 2003b). Irradiations were carried out within the Risø reader using the ^{90}Sr/^{90}Y beta source.

In addition, 150-180 μm and 212-250 μm grains were separated using heavy liquids of densities 2.58 and 2.62 g.cm^{-3}. The grains within this density range were assumed to be NaF. They were used together with the equivalent KF grains for studying the relative thermal stability of the IRSL signals from these two materials. The IRSL signals from each NaF grain were measured in the same way as for the individual KF grains. The efficiency of the heavy liquid separation of NaF and KF grains was tested by measuring the K content of the two fractions using the Risø GM-25-5 beta counter (Bøtter-Jensen and Mejdahl, 1988). The K content of the KF fraction was found to be in the range of 11.4-14.3% for different grain sizes of Sm1 and 10.2-12.2% for HLD3 (Li et al., 2008b), and the NaF fraction of HLD3 had a K content of 2.4±0.2%. Given that the theoretical K content of a pure K-feldspar is ~14% (Huntley and Baril, 1997), the beta counting results indicated that the KF grains were concentrated in the fraction with a density that was less than 2.58 g.cm^{-3}, while a range of feldspar compositions are likely to be present in the fraction with a density between 2.58 and 2.62 g.cm^{-3}, but all sharing the common trait of a low K content.

3. Dose rate calibration for single grain measurement

There have been several studies on the uniformity of the dose rate from a $^{90}Sr/^{90}Y$ beta source for short source-to-target distances. Using single grains placed on a conventional aluminium disc, Spooner and Allsop (2000) showed that the dose rate decreased by as much as 10% from the centre of the target disc to 5 mm from the centre for their beta sources. For their readers, Veronese et al. (2007) and Ballarini et al. (2006) made a study of source uniformity using grains mounted in a single-grain disc. Therefore, it was essential for us to undertake calibration for individual holes in the single-grain disc in order to know the dose delivered to individual grains during the experimental procedures undertaken to obtain the equivalent dose. Only once this has been checked is it then possible to go on and obtain the dose rates for grains of different sizes. As in the case of measurement of aliquots containing several thousand grains, this calibration was carried out using quartz supplied by Risø National Laboratory, Denmark which they had extracted from a sediment collected from Jutland, annealed at 500°C and then packed into a glass flat-pack prior to irradiating (5.10 ± 0.06 Gy) in the dark using a ^{137}Cs gamma source. The quartz was sieved to obtain fractions with diameters 90-125, 125-150, 150-180, 180-212 and 212-250 μm.

Two sets of measurements were undertaken. In the first, ten discs were measured using the single grain system to determine the dose rate specific to each grain position. This was undertaken to assess whether there was significant variability in the beta dose delivered to grains in different positions on the disc. A total of 1000 grains had their OSL signal (OSL detection through a U-340 filter) measured using the green-emitting laser (532 nm) in the same Risø TL/OSL reader. Of these, 981 passed the rejection criteria for the standard single aliquot regenerative dose (SAR) protocol (Murray and Wintle, 2000), giving between 7 and 10 calibration values for each position. The weighted mean was calculated for each position, and the standard error calculated as the uncertainty. These values were then used to calculate the central value of dose rates using the central age model (Galbraith et al., 1999). A small over-dispersion (OD) of 3.6% was obtained from the data set. This suggests that the spatial heterogeneity of the dose rate across the single-grain disc would bring a ~3.6% over-dispersion to all D_e distributions obtained using the same reader. To illustrate the spatial distribution of the dose rate across the single-grain disc, the grains with a dose rate inside and outside two sigma of the central value are

shown in different colours in Fig. 1(a). It is shown that ~85% of the area has a similar dose rate, consistent within two sigma of the central value.

A second set of measurements was undertaken to precisely calculate the dose rate for the different grain sizes. To improve the precision, all grains on a single grain (SG) disc were measured simultaneously using blue LEDs (470 nm) as the stimulation light source, rather than the green (532 nm) emission from the laser. The standard SAR protocol (Murray and Wintle, 2000) was applied, and at least 10 discs for each grain size were measured to calculate the dose rate. Fig. 1(b) shows the experimentally determined dose rates as a function of the average grain diameter. The same dose rate was found for grain sizes from 90 to 250 μm when SG discs were used. Therefore, in this study of SG measurements, the same dose rate was applied to all grain sizes. It should be noted that the data in Fig. 1(b) differ from the results obtained previously using single aliquot (SA) discs; Li et al. (2007) found that the dose rate was slightly dependent on grain sizes in the range from 63 to 250 μm. This is probably due to the different irradiation geometry for grains lying on (SA) or within (SG) the two types of discs, e.g. different source-to-sample distance, different structure of discs and different grain position relative to the disc surface.

4. Thermal stability of IRSL signals

Previous studies have shown that IRSL signals from NaF are less thermally stable than those from KF (Li and Wintle, 1992; Tso et al., 1996) when the same detection window (blue-violet emission) is used for both NaF and KF. In comparison to the optically stimulated luminescence signals from quartz, the IRSL signals from feldspars do not come from a single trap. The IRSL signals are derived from a distribution of traps, each with a characteristic thermal stability; thus curve fitting cannot be used to obtain a thermal activation energy for the signal.

In this study, sample Sm1 gave a D_e value of 21.5±1.5 Gy for single aliquot measurements on NaF ($2.58 < \rho < 2.62$ g.cm^{-3}), a value which is significantly lower than that of 37.7±0.5 Gy obtained for the KF fraction ($\rho < 2.58$ g.cm^{-3}). Such a large discrepancy between the D_e values from NaF and KF cannot be explained by the difference between their internal dose rates. Assuming K contents of 2% (based on the measured value for HLD3) and 13% (based on the most likely value as measured by Zhao and Li (2005)) for the NaF and KF fractions,

respectively, IRSL ages of 6.2±0.4 ka and 8.9±0.1 ka are calculated. A possible reason for the discrepancy is that the IRSL signal from the NaF fraction has lower thermal stability than that of the KF fraction. This was further investigated using pulse annealing experiments on single grains in which the IRSL signals are measured after heating to temperatures that result in depletion of electrons in the traps giving rise to the IRSL signals.

4.1 Pulse annealing characteristics of NaF and KF

A pulse annealing test (Duller, 1994; Li et al., 1997) was conducted to study the stability of the IRSL signals from NaF grains and KF grains extracted using heavy liquids of density 2.58 and 2.62 g.cm^{-3}. Pulse annealing, using the experimental sequence listed in Table 1, was undertaken on 200 single grains (150 to 180 μm diameter) from each sample (Sm1 and HLD3) using the single grain system, 100 grains from the KF fraction and 100 grains from the NaF fraction. The grains first had their natural IRSL removed using the IR laser for 1.8 s. After that, the grains were given a regenerative dose (D=42 Gy). They were then heated to a temperature (T), cooled immediately (termed a cut-heat) and the remaining IRSL signal (L_i) was then measured. Following each measurement of L_i, the grains were given a test dose (D_T=14 Gy) and preheated at 200ºC for 10 s before the test dose IRSL (T_i) was measured to monitor the sensitivity related to L_i. This procedure was repeated, but increasing the temperature T from 200 to 420°C in steps of 20°C.

The normalized corrected IRSL signal (L_i/T_i) as a function of the cut-heat temperature (T) for KF grains (filled squares) and NaF grains (filled triangles) is shown for sample HLD3 (Fig. 2(a)) and Sm1 (Fig. 2(b)). The data points were obtained by taking the sum of L_i/T_i for each of the 100 grains measured. For HLD3, 63 of the 100 grains in the KF fraction gave IRSL signals higher than 3σ of the background, but only 25 of the 100 grains from the NaF fraction gave IRSL signals higher than 3σ of the background. For those KF grains, their individual pulse annealing curves are similar, as shown by the small standard errors for the data set (most of the error bars are within the symbols), suggesting that any variation in chemical composition due to perthitic structures has a limited impact on their luminescence properties. A distinct difference can be seen between the pulse annealing curves for KF and NaF grains. Up to 80% of the IRSL signal from KF remained after heating to 300°C, whereas only 50% of the IRSL signal from the NaF

grains was left by heating to the same temperature. This result confirms the conclusion that the IRSL signal from NaF uses a higher proportion of shallow traps than the IRSL from KF (Li and Wintle, 1992). No distinct difference was observed between NaF and KF for the sensitivity changes during pulse annealing; both sensitivities (T_i) increased slightly from 200 to 280°C, decreased by about 40% from 300 to 400°C and then reached a stable level from 400 to 420°C. It is thus unlikely that the difference between the pulse annealing curves for KF and NaF (Figs. 2(a) and (b)) is a result of failure in sensitivity correction.

4.2 Pulse annealing to distinguish NaF and KF

The results in Fig. 2 suggest that the KF grains can be distinguished from NaF grains based on the different annealing profiles of their IRSL signals and that the individual annealing profiles from the individual grains separate into two distinct groups (NaF and KF). This provides a useful tool to test the validity of the assumption that the IRSL signal measured from KF fractions is dominated by the signal from KF grains. In this test, the KF fractions of two grain sizes (125-150 and 212-250 μm) from sample Sm1 were investigated. The pulse annealing test outlined in Table 1 was then carried out with D=42 Gy and D_T=14 Gy.

Among the 100 grains of size 125-150 μm investigated, there are 58 grains giving measurable IRSL signals (higher than 3σ of background), but only one grain from the 58 grains has a thermally unstable IRSL signal (Fig. 3(a)). The D_e measurement for this grain also gave a relatively low D_e value of 20±2.7 Gy compared to the average D_e value of all grains of 32.7±0.3 Gy. The natural IRSL signal from this grain is only 1.1% of the total natural IRSL from all grains on the whole disc. For the 212-250 μm grains, there are 47 grains giving measurable IRSL signals (higher than 3σ of background) out of the 100 grains, and also only one grain from the 47 grains has a thermally unstable IRSL signal (Fig. 3(b)). No acceptable D_e was obtained for this grain due to its weak natural IRSL signal.

As the IRSL signal from the NaF fraction is thermally unstable when compared to that from the KF fraction, it is likely that those grains with unstable IRSL signals (Fig. 3(a) and (b)) identified in the KF fractions might be low-potassium feldspar grains due to the imperfect separation using heavy liquid. However, since there is only 1 grain with thermally unstable IRSL

out of the 58 grains in the case of the 125-150 μm grains (Fig. 3(a)), it is concluded that the IRSL signal measured from the KF fraction is dominated by thermally stable signals, which are mainly from high-potassium feldspar grains. It is thus concluded that a high value of K content for KF fractions (e.g. 13±1% as discussed by Huntley and Baril (1997) and Zhao and Li (2005)) should be used for estimation of the internal dose rates in iIRSL dating (Li et al., 2007, 2008b).

5 D_e determination using single KF grains

From the pulse annealing study, it seems that for these samples there are only a small number (~2%) of NaF grains in the KF separates employed for multiple grain iIRSL dating. These grains contribute <2% of the IRSL signal and therefore will have only a very small impact on the measured D_e values. However, equivalent studies of OSL signals of single quartz grains (Jacobs et al., 2008) have indicated that single grain measurements provide a way to reject grains with aberrant behaviour, thus increasing the precision of ages. A similar approach, i.e. rejecting grains with undesirable properties and then combining the resulting data to obtain a more accurate and precise value of the D_e for each grain size used in the iIRSL procedure, might be feasible for individual KF grains. In this section, we present D_e determinations of several hundred grains for each grain size separated from sample Sm1 and investigate the impact of applying various rejection criteria.

5.1 Measurement procedure

A modified SAR procedure (Auclair et al., 2003; Blair et al., 2005) was used for D_e determination of single grains of KF. The same preheat condition (10 s at 260°C) was used ahead of both the main IRSL measurement (L, due to the natural and the regenerative dose) and the test dose IRSL measurement (T). A typical IRSL decay curve and dose response curve are shown in Fig. 4(a) and (b), respectively. The IRSL signal was measured at 60°C for 1.8 s. The signal used for construction of the dose response curves and calculation of the D_e values was that observed in the first 0.1 s after the laser was switched on, with the signal observed in the last 0.1 s of stimulation time being subtracted.

5.2 Variability of the single grain IRSL signal

Although many hundreds of grains were measured for each grain size, not all the grains gave the same signal. In Fig. 5 the cumulative IRSL light sum is plotted as a function of the proportion of the brightest grains for 100 naturally irradiated KF grains. It can be seen that one grain is very bright, giving rise to 18% of the light from the 100 grains; it and the next 5 brightest grains give rise to 40% of the light from the 100 grains (cf. McFee and Tite, 1998). Removing these six grains from the data set and replotting (Fig. 5) shows that all the remaining grains contribute to the total light sum. Of the remaining 94 grains, ~60% contribute 80% of the light sum.

Fig. 5 is in strong contrast to the results from quartz where fewer than 20% of the grains typically contribute more than 80% of the total OSL signal (e.g. Duller et al., 2000; McCoy et al., 2000; Thomsen et al., 2002; Duller et al., 2003). The more even distribution of luminescence output suggests that it is advantageous to use KF, rather than quartz, for D_e determination, especially in single grain measurements.

5.3 Dose recovery test

To test the reliability of the SAR method described above, a 'dose recovery' experiment (Wintle and Murray, 2006) was carried out using 300 grains from the 180-212 μm fraction of sample Sm1. This was achieved by first zeroing the natural signal using the IR laser and then giving a dose of 32 Gy to the grains. The given dose was then treated as an 'unknown' dose and measured using the same SAR procedure as used in 'natural dose' measurements. Rejection criteria are needed to select reliable D_e values, and are similar to those suggested for quartz single grain measurements (Jacobs et al., 2006). Grains were rejected if:

(1) The recycling ratio is outside the range of 1.0±0.1, as originally suggested by Murray and Wintle (2000); this criterion demonstrates the accuracy of the sensitivity correction in the SAR procedure.

(2) The natural signal (L_N) is less than 3 times the standard deviation of the background; this criterion is related to the instrumental detection limit (Thomsen et al., 2006).

(3) The relative error of the test dose IRSL (T_N) is larger than 20%; this criterion is to ensure that the sensitivity correction is not hampered by large uncertainty in T_N.

(4) There is an 'abnormal' dose response curve. For some grains, although the IRSL signal has a high sensitivity and an acceptable recycling ratio, the corrected IRSL signals are found to be very scattered and cannot be fitted with any line or curve.

(5) The response to zero dose (usually expressed as the ratio between the sensitivity corrected IRSL signals for the zero dose and natural dose, and termed the recuperation ratio) is greater than 10% of the natural response.

Of the 300 grains measured in the dose recovery experiment, 117 grains passed criteria 1-4. Fig. 6 shows the radial plot of the 'recovered doses' for these 117 grains. Of these grains, seventy-two had recuperation greater than 10% and using the central age model they yielded a recovered dose of 25.1±0.6 Gy only 78% of the given laboratory dose. The other 45 grains had recuperation less than 10% and the recovered dose for these (30.1±0.6 Gy) is much closer to the given dose (94%). We conclude that selecting grains with recuperation less than 10% is essential to obtain accurate dose recovery, but note that only a small proportion, 45 out of 300 grains (15%), passes all five rejection criteria.

5.4 Recuperation in IRSL signals of KF

The observation that recuperation above 10% is common amongst these single grain measurements is surprising since single aliquot measurements on the same sample do not show this. We observed a small amount (~2%) of recuperation in single aliquot measurements of sample Sm1. To compare the recuperation of single aliquot and single grain results, the signals from all 100 grains from a SG disc containing 212-250 μm diameter grains were summed to create a synthetic single aliquot and these used to calculate a dose response curve. High recuperation (10.1%) was observed for this dataset, and similar high recuperation values were observed for all synthetic aliquots composed of single grain measurements.

Recuperation of IRSL in single grain measurements was investigated by checking whether there is a relationship between D_e values and the amount of recuperation. For the five grain sizes

separated from Sm1, between 300 and 700 grains were measured using a SAR procedure to determine their D_e (Table 2, column 2). Fig. 7 shows the relationship between the percentage recuperation and the D_e values for those grains remaining after applying the first four rejection criteria (see Table 2, N1, column 3). A wide range of recuperation values is found within each grain size fraction, with values above 20% not being uncommon. The weighted mean of the D_e value for 90-125 μm grains with recuperation higher than 10% is 30.3±0.4 Gy (n=130), while that for grains with recuperation less than 10% is 32.3±0.3 Gy (n=130). This increase in D_e for grains with lower recuperation is similar to that observed in the dose recovery experiment (Fig. 6).

To see whether the 10% criterion is sufficient to eliminate grains which underestimate D_e, we reduced the acceptance criterion such that recuperation was less than 5%. This resulted in a D_e value of 33.2±0.9 Gy (n=29), similar to that obtained for a threshold of 10% recuperation. However application of the 5% threshold resulted in a significant reduction in the number of grains, by a factor of four, and this has led us to maintain the threshold at 10%. The number of grains passing all five rejection criteria is given in Table 2 (N2, column 4), showing that this was between 16% and 26% of the total number of grains measured. This proportion of acceptable grains is generally higher than the published results obtained for sedimentary quartz grains (Duller et al., 2000; Yoshida et al., 2000; Jacobs et al., 2003; Duller, 2006; Jacobs et al., 2006), but is low considering the number of grains which gave a measurable IRSL signal (Fig. 5).

5.5 D_e distributions from KF grains

For Sm1, the D_e values obtained for different grain sizes of KF after applying the rejection criteria are shown as radial plots (Galbraith, 1988; Galbraith et al., 1999) in Fig. 8(a)-(e). A number of D_e values lie outside the ±2σ range of the weighted mean value (shown as the shaded band in each figure), suggesting that the D_e distributions are over-dispersed. For the five grain sizes, OD values from 0.13 to 0.19 are obtained (Table 1), similar to those reported for quartz grains from aeolian sediments (e.g. Jacobs et al., 2006). This confirms the suggestion made in section 2 that these grains were well bleached at deposition, and that therefore the iIRSL method is applicable.

5.6 Isochron dating based on single grain IRSL measurements

To obtain a single value of D_e for each grain size for calculation of the age, different statistical models can be used to combine the D_e values for the accepted grains, namely the 'weighted mean', 'common age model' and the 'central age model' (Galbraith et al., 1999). The 'weighted mean' and the 'common age model' assume that all grains have received the same dose and the variation in D_e values can be accounted for by the instrumental uncertainty, counting statistics and curve fitting. The difference between the 'weighted mean' and the 'common age model' D_e value is that the former assumes that D_e is normally distributed whereas the latter assumes that $\ln(D_e)$ is normally distributed. On the other hand, the 'central age model' assumes that the distribution of $\ln(D_e)$ is not consistent with a single population but the D_e values are randomly distributed around a central value with a variation that cannot be accounted for by measurement uncertainties.

These different ways of calculating the value of D_e have been used to analyze the data sets in Fig. 8, and the results for the different grain sizes are listed in Table 2. The D_e values obtained from different models differ slightly but are consistent with each other within 2σ (Fig. 8). The weighted mean consistently gave the highest dose values and the central age model gave the lowest. The D_e values obtained using all age models increase as the grain size increases, consistent with the results obtained using the single aliquot (multiple grain) measurements (Li et al., 2008b) as shown in Table 2 (last column).

Fig. 9 shows the iIRSL plots using the single grain D_e values calculated using different statistical models. From the data sets, it seems that the central age model gives better linearity in the data points (R^2=0.98 compared to 0.93 and 0.89 for the common age model and weighted mean, respectively). Isochron ages of 10.6±1.8 ka, 10.5±1.4 ka and 9.9±1.7 ka are obtained using the weighted mean, common age and central age models, respectively (Fig. 9(a), (b) and (c)); these all agree with the isochron age of 10.9±1.5 ka obtained using single aliquot IRSL measurements (Li et al., 2008b) and the quartz OSL age of 9.1±0.5 ka. Given that there is over-dispersion observed in the D_e distribution (Fig. 8), the central age model is taken as providing the best estimation of the D_e.

6 Discussions

The iIRSL method is crucially dependent upon calculation of the internal dose rate applicable to the grains responsible for the IRSL signal used to determine the D_e for each grain size. In multiple grain iIRSL measurements it has been assumed that the IRSL signal originates from KF grains with a K content of 13±1%, following the work of Huntley and Baril (1997). The pulse annealing characteristics of grains taken from the NaF fraction ($2.58 < \rho < 2.62$ g.cm^{-3}) and grains from the KF fraction ($\rho < 2.58$ g.cm^{-3}) from two samples as obtained using heavy liquids are quite different (Fig.2(a) and (b)) in spite of the potential for complex variations in major element chemistry within feldspars; these confirm observations made for other samples by Li et al. (1997). This difference in behaviour is attributed to the different thermal stabilities of KF and NaF. Single grain pulse annealing measurements for Sm1 demonstrate that less than 2% of the IRSL signal from the KF separates originates from grains which appear to have NaF pulse annealing properties; the remaining 98% of the IRSL signal comes from grains which have the thermal stability attributed to KF. This dominance of KF grains in the fraction that has a density of < 2.58 g.cm^{-3} is consistent with the measured K concentration for these KF separates (11.4-14.3%), which itself is close to the theoretical K content for pure K-feldspar.

Although the separation of KF feldspars from desert samples from China (e.g. Sm1 and HLD3) using heavy liquid has been very effective, greater contamination with NaF may be possible for other types of sample with fewer KF grains. For those samples, single grain measurements provide the potential to overcome imperfect physical separation and to improve calculation of D_e by allowing grains which are not KF, or which have inappropriate luminescence properties to be excluded; the signals from the remaining grains can then be combined together to create synthetic aliquots. This approach is an attractive proposition because a large proportion of KF grains emit a measurable IRSL signal (Fig. 5) and thus relatively few grains would need to be measured to obtain good statistics. However, when the rejection criteria based upon those used in OSL dating of quartz are applied to the KF single grain data, a large number of grains are rejected (Table 2). Surprisingly, the criterion that leads to rejection of the largest number of grains is recuperation. Single aliquot measurements for Sm1 have recuperation values of ~2%, but the average recuperation for single grain measurements is ~10%, with values of 20% or higher occurring frequently (Fig. 7). The two optical stimulation sources used for these two sets of measurements have different wavelengths (Single aliquot LEDs: 880±80 nm;

Single grain laser: 830Δ10 nm) and different power densities (Single aliquot LEDs: 150 mW.cm^{-2}; Single grain laser: 400 W.cm^{-2}). At this stage we are not clear why such a large difference in recuperation is observed, but the effect is most likely to be due to the different amount of energy deposited in the grains during the IRSL measurement (see Bøtter-Jensen and Murray, 1999) and thus the different extent to which the IRSL signal is removed in each cycle.

Analysis of the data from the dose recovery experiment (Fig. 6) demonstrated that those grains with recuperation greater than 10% had to be excluded in order to recover the given laboratory dose. Grains with higher recuperation yielded D_e values that are, on average, too low. The same pattern was also observed for the D_e data obtained from different grain sizes of Sm1 (Fig. 7). After excluding grains with recuperation greater than 10% and applying the other rejection criteria, between 16 and 26% of the grains which were measured gave acceptable D_e values. The distribution of D_e values for different grain sizes is similar, with over-dispersion values from 0.13 to 0.19 (Fig. 8). Such values cannot be explained by the heterogeneity of the beta dose rate in the single-grain measurements, which can only result in a small over-dispersion of ~3.6% (see section 3). From studies of quartz single grains, similar values of over-dispersion would be expected for samples that were well bleached at deposition (e.g. Olley et al., 2004). The causes of over-dispersion in quartz are not well understood, but it is thought that microdosimetry plays a major role. For KF grains, the total dose to the grains consists of both external and internal doses, and so the impact of variation in the external dose rate would be expected to have a smaller total impact than quartz. However, for the grain sizes used here, the external dose is responsible for ~85% of the total dose, and so over-dispersion due to this cause would still be important.

7 Conclusions

Pulse annealing measurements on single grains separated from Sm1 by density (ρ <2.58 g.cm^{-3}) have demonstrated that over 98% of the IRSL signal measured from these materials originates from grains whose annealing profiles suggest that they are high potassium feldspars. This finding supports previous microprobe measurements giving high K concentrations for these separates (Zhao and Li, 2005).

High recuperation of the IRSL signal was observed for many grains in the single grain IRSL measurements, even though recuperation was low in single aliquot measurements from the same separation. After removing grains with high recuperation, D_e values were obtained which yielded an iIRSL age consistent with multiple grain measurements, thus suggesting that this method may be valuable. However, further work would be required to understand why such high recuperation values are observed in single grain IRSL measurements.

The iIRSL age based on single grain IRSL measurements agrees with that based on previous multi-grain measurements. However, the single grain IRSL measurements did not result in a final age with a lower uncertainty when compared with the multiple grain measurements. It is thus concluded that the most effective way of applying the iIRSL method is by using multiple grain IRSL measurements on KF with K contents in excess of ~10%. However, for samples having difficulty in separation of KF grains, single grain D_e measurements in combination with pulse annealing test could be used as a screening procedure to reject contaminant NaF grains.

Use of a value of 13±1% for the K content in the iIRSL method when applied to either multiple grain or single aliquot measurements for these samples resulted in ages compatible with other chronological evidence. However, studies should be undertaken to explore the relationship between the microdosimetry and luminescence behaviour of feldspar grains. In particular, the U and Th contents of the individual grains should be measured (e.g. by laser-ablation mass-spectrometric techniques) and the K concentrations mapped to check for perthitic structures.

Acknowledgements

The authors thank Professor Andrew Murray for help with gamma-irradiation of the heated quartz grains. Dr. David Sanderson and two anonymous referees are appreciated for their constructive comments. This study is financially supported by a grant to SHL from the Research Grant Council of the Hong Kong Special Administrative Region, China (Project no. 7035/06P, 7035/07P and 7028/08P).

References

Auclair, M., Lamothe, M., Huot, S., 2003. Measurement of anomalous fading for feldspar IRSL using SAR. *Radiation Measurements* **37**, 487-492.
Ballarini, M., Wintle, A.G., Wallinga, J., 2006. Spatial variation of dose rate from beta sources as measured using single grains. *Ancient TL* **24**, 1-8.
Baril, M.R., Huntley, D.J., 2003. Infrared stimulated luminescence and phosphorescence spectra of irradiated feldspars. *Journal of Physics-Condensed Matter* **15**, 8029-8048.
Blair, M.W., Yukihara, E.G., McKeever, S.W.S., 2005. Experiences with single-aliquot OSL procedures using coarse-grain feldspars. *Radiation Measurements* **39**, 361-374.
Bøtter-Jensen, L., Andersen, C.E., Duller, G.A.T., Murray, A.S., 2003a. Developments in radiation, stimulation and observation facilities in luminescence measurements. *Radiation Measurements* **37**, 535-541.
Bøtter-Jensen, L., McKeever, S.W.S., Wintle, A.G., 2003b. *Optically Stimulated Luminescence Dosimetry*. Elsevier Amsterdam. 355pp.
Bøtter-Jensen, L., Mejdahl, V., 1988. Assessment of beta dose-rate using a GM multicounter system. *Nuclear Tracks and Radiation Measurements* **14**, 187-191.
Bøtter-Jensen, L., Murray, A.S., 1999. Developments in optically stimulated luminescence techniques for dating and retrospective dosimetry. *Radiation Protection Dosimetry* **84**, 307-315.
Clark, P.A., 1994. Isochron methods for luminescence dating in archaeology. Unpublished Ph.D. thesis, Glasgow University.
Duller, G.A.T., 1994. A new method for the analysis of infrared stimulated luminescence data from potassium feldspars. *Radiation Measurements* **23**, 281-285.
Duller, G.A.T., 2006. Single grain optical dating of glacigenic deposits. *Quaternary Geochronology* **1**, 296-304.
Duller, G.A.T., Bøtter-Jensen, L., Murray, A.S., 2000. Optical dating of single sand-sized grains of quartz: sources of variability. *Radiation Measurements* **32**, 453-457.
Duller, G.A.T., Bøtter-Jensen, L., Murray, A.S., 2003. Combining infrared- and green-laser stimulation sources in single-grain luminescence measurements of feldspar and quartz. *Radiation Measurements* **37**, 543-550.
Fain, J., Soumana, S., Montret, M., Miallier, D., Pilleyre, T., Sanzelle, S., 1999. Luminescence and ESR dating - Beta-dose attenuation for various grain shapes calculated by a Monte-Carlo method. *Quaternary Science Reviews* **18**, 231-234.
Fleming, S.J., Stoneham, D., 1973. The subtraction technique of thermoluminescent dating. *Archaeometry* **15**, 229-238.
Galbraith, R., 1988. Graphical display of estimates having differing standard errors. *Technometrics* **30**, 271-281.
Galbraith, R.F., Roberts, R.G., Laslett, G.M., Yoshida, H., Olley, J.M., 1999. Optical dating of single and multiple grains of quartz from Jinmium rock shelter, northern Australia, part 1, Experimental design and statistical models. *Archaeometry* **41**, 339-364.
Huntley, D.J., Baril, M.R., 1997. The K content of the K-feldspars being measured in optical dating or in thermoluminescence dating. *Ancient TL* **15**, 11-13.
Huntley, D.J., Hancock, R.G.V., 2001. The Rb contents of the K-feldspars being measured in optical dating. *Ancient TL* **19**, 43-46.
Jacobs, Z., Duller, G.A.T., Wintle, A.G., 2003. Optical dating of dune sand from Blombos Cave, South Africa: II - single grain data. *Journal of Human Evolution* **44**, 613-625.
Jacobs, Z., Duller, G.A.T., Wintle, A.G., 2006. Interpretation of single grain D_e distributions and

calculation of D_e. *Radiation Measurements* **41**, 264-277.
Jacobs, Z., Roberts, R.G., Galbraith, R.F., Deacon, H.J., Grün, R., Mackay, A., Mitchell, P., Vogelsang, R., Wadley, L., 2008. Ages for the Middle Stone Age of Southern Africa: Implications for Human Behavior and Dispersal. *Science* **322**, 733-735.
Li, S.H., Sun, J.M., Zhao, H., 2002. Optical dating of dune sands in the northeastern deserts of China. *Palaeogeography Palaeoclimatology Palaeoecology* **181**, 419-429.
Li, B., Li, S.H., Wintle, A.G., 2008a. Overcoming environmental dose rate changes in luminescence dating of waterlain deposits. *Geochronometria* **30**, 33-40.
Li, B., Li, S.H., Wintle, A.G., Zhao, H., 2007. Isochron measurements of naturally irradiated K-feldspar grains. *Radiation Measurements* **42**, 1315-1327.
Li, B., Li, S.H., Wintle, A.G., Zhao, H., 2008b. Isochron dating of sediments using luminescence of K-feldspar grains. *Journal of Geophysical Research-Earth Surface* **113**, F02026, doi:02010.01029/02007JF000900. .
Li, S.H., Tso, M.Y.W., Wong, N.W.L., 1997. Parameters of OSL traps determined with various linear heating rates. *Radiation Measurements* **27**, 43-47.
Li, S.H., Wintle, A.G., 1992. A global view of the stability of luminescence signals from loess. *Quaternary Science Reviews* **11**, 133-137.
McCoy, D.G., Prescott, J.R., Nation, R.J., 2000. Some aspects of single-grain luminescence dating. *Radiation Measurements* **32**, 859-864.
McFee, C.J., Tite, M.S., 1998. Luminescence dating of sediments - The detection of high equivalent dose grains using an imaging photon detector. *Archaeometry* **40**, 153-168.
Mejdahl, V., 1983. Feldspar inclusion dating of ceramics and burnt stones. *PACT* **9**, 351-364.
Murray, A.S., Wintle, A.G., 2000. Luminescence dating of quartz using an improved single-aliquot regenerative-dose protocol. *Radiation Measurements* **32**, 57-73.
Olley, J.M., Pietsch, T., Roberts, R.G., 2004. Optical dating of Holocene sediments from a variety of geomorphic settings using single grains of quartz. *Geomorphology* **60**, 337–358
Readhead, M.L., 2002. Absorbed dose fraction for ^{87}Rb β particles. *Ancient TL* **20**, 25-27.
Spooner, N.A., Allsop, A., 2000. The spatial variation of dose-rate from Sr-90/Y-90 beta sources for use in luminescence dating. *Radiation Measurements* **32**, 49-56.
Thomsen, K.J., Bøtter-Jensen, L., Denby, P.M., Moska, P., Murray, A.S., 2006. Developments in luminescence measurement techniques. *Radiation Measurements* **41**, 768-773.
Thomsen, K.J., Bøtter-Jensen, L., Murray, A.S., Solongo, S., 2002. Retrospective dosimetry using unheated quartz: A feasibility study. *Radiation Protection Dosimetry* **101**, 345-348.
Tso, M.Y.W., Wong, N.W.L., Li, S.H., 1996. Determination of lifetime of infrared stimulated signals from potassium and sodium feldspars. *Radiation Protection Dosimetry* **66**, 387-389.
Veronese, I., Shved, V., Shishkina, E.A., Giussani, A., Göksu, H.Y., 2007. Study of dose rate profile at sample disks in a Risø OSL single-grain attachment system. *Radiation Measurements* **42**, 138-143.
Wintle, A.G., Murray, A.S., 2006. A review of quartz optically stimulated luminescence characteristics and their relevance in single-aliquot regeneration dating protocols. *Radiation Measurements* **41**, 369-391.
Yoshida, H., Roberts, R.G., Olley, J.M., Laslett, G.M., Galbraith, R.F., 2000. Extending the age range of optical dating using single 'supergrains' of quartz. *Radiation Measurements* **32**, 439-446.
Zhao, H., Li, S.H., 2002. Luminescence isochron dating: A new approach using different grain

sizes. *Radiation Protection Dosimetry* **101**, 333-338.
Zhao, H., Li, S.H., 2005. Internal dose rate to K-feldspar grains from radioactive elements other than potassium. *Radiation Measurements* **40**, 84-93.

Table 1: Sequence of the pulse annealing test of the stability of single grain IRSL signals.

Step	Treatment	Observation
1	Give a regeneration dose, D	
2	Cut-heat to T°C (200-420°C)	
3	Single grain IRSL measurement at 60°C, 1.8 s	L_i
4	Give a test dose, D_T	
5	Preheat at 200°C for 10 s	
6	Single grain IRSL measurement at 60°C, 1.8 s	T_i
7	Return to step 1, T=T+20°C	

Table 2: Summary of the single grain IRSL D_e results for sample Sm1. The single aliquot results of Li et al. (2008b) are also shown for comparison in the last column. N is the total number of grains measured, N1 is the number remaining after application of the first four rejection criteria listed in the text, and N2 is the number remaining after applying the additional rejection criterion for recuperation.

Grain size, μm	N	N1	N2	Weighted Mean (Gy)	Common age (Gy)	Central age (Gy)	Over-dispersion	Single aliquot D_e (Gy)
90-125	500	260	130 (26%)	32.3±0.3	31.8±0.3	31.8±0.5	0.13±0.01	33.0±0.3
125-150	700	240	109 (16%)	33.9±0.4	33.3±0.4	32.3±0.6	0.15±0.01	33.5±0.4
150-180	500	289	107 (21%)	35.5±0.3	34.8±0.3	33.5±0.7	0.19±0.01	35.1±0.6
180-212	300	80	52 (17%)	36.4±0.5	35.7±0.5	34.6±1.0	0.17±0.02	35.4±0.4
212-250	400	140	75 (19%)	36.5±0.3	36.1±0.3	35.8±0.7	0.14±0.02	37.7±0.5

Figure captions

Figure 1: Source calibration data (a) Spatial distribution of the dose rate of different grain positions shown in a 10x10 pattern. The positions with dose rates consistent within two sigma of the central value are shown in red. The positions with dose rates outside two sigma of the central value are shown in green (higher dose rates) and blue (lower dose rate), respectively. (b) Dose rate calibration results for different grain sizes using single grain (SG) discs. The data set was normalized to 1 at 90-125 μm.

Figure 2: Pulse annealing results for K-feldspar grains (filled squares) and NaF grains (filled triangles) taken from separates obtained with heavy liquids for sample HLD3 (a) and Sm1 (b). Each data point is the average of measurements on 100 grains. The data sets were normalized to the first point for the cut-heat at 200ºC.

Figure 3: Pulse annealing results using K-feldspar grains of 125-150 μm (a) and 212-250 μm (b) from Sm1. Filled squares are the average of 100 grains in each case. In each figure the pulse annealing curve for the one unstable grain identified in each set of measurements is shown by the open triangle.

Figure 4: (a) Single grain IRSL decay curve measured at 60°C for 1.8 s. (b) A dose response curve for a single grain of sample Sm1 fitted with a saturating exponential function.

Figure 5: Distribution of IRSL signal intensity from 100 single grains of K-feldspar from sample Sm1 (filled diamonds). Data are plotted as the proportion of the total light sum that originates from the specified percentage of the brightest grains. Empty squares show the distribution after removing the first six grains from the complete data set.

Figure 6: Radial plot of the doses calculated for grains (diameter 180-212 μm) given a laboratory dose of 32 Gy (horizontal solid line) which have passed the first four rejection criteria listed in the text. Grains with recuperation greater than 10% are shown as open triangles and have a calculated dose of 25.1±0.6 Gy (lower solid line). Grains with recuperation less than 10% are shown as filled circles and have a calculated dose of 30.1±0.6 Gy (grey bar).

Figure 7: The relationship between the recuperation and the D_e values for different grains of different grain sizes (90-125, 125-150, 150-180, 180-212 and 212-250 μm) for sample Sm1. The D_e values are for those grains passing the first four rejection criteria (see text).

Figure 8: Radial plot of IRSL D_e values for K-feldspar grains of different grain sizes from sample Sm1. Full circles and empty circles are those values that fall within and outside ±2σ of the 'weighted mean' value given in Table 1. Red, green and blue lines represent the values obtained using "weighted mean", "common age model" and "central age model", respectively.

Figure 9: Results of isochron dating for sample Sm1 using single grain results based on different age models, (a) weighted mean; (b) common age; (c) central age. The experimental data for K-feldspars were fitted by a linear function using the least squares method. The dashed line, representing the external dose rate with allowance being made for grain size, has as its starting point the extrapolation of the line fitted through the experimental points (see Li et al (2008b) for a detailed description). The internal dose rate was calculated by assuming a K-content of 13±1% and a Rb-content of 400 $\mu g.g^{-1}$ (Huntley and Baril, 1997; Huntley and Hancock, 2001; Zhao and Li, 2005; Li et al., 2007). The values of beta absorption coefficient as a function of grain size for the decay of ^{40}K are taken from Fain et al (1999) by interpolating between the values they provided. The values of the absorbed dose from ^{87}Rb are taken from Readhead (2002).

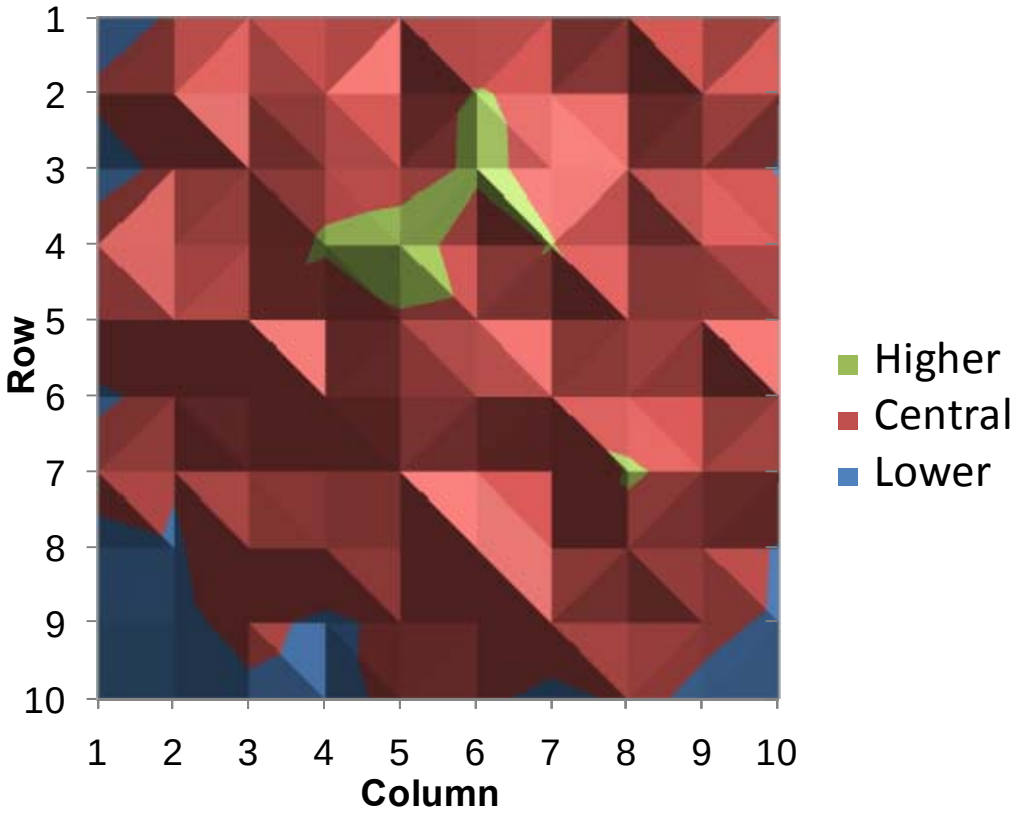

Figure 1 (a)

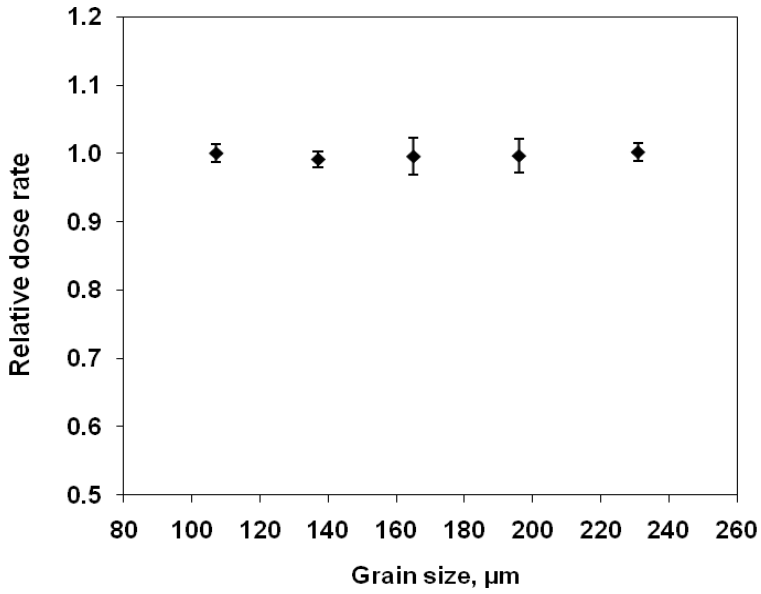
1.2
1.1
1.0
0.9
0.8
0.7
0.6
0.5
Relative dose rate
80
100
120
140
160
180
200
220
240
260
Grain size, µm

Figure 1(b)

(a)

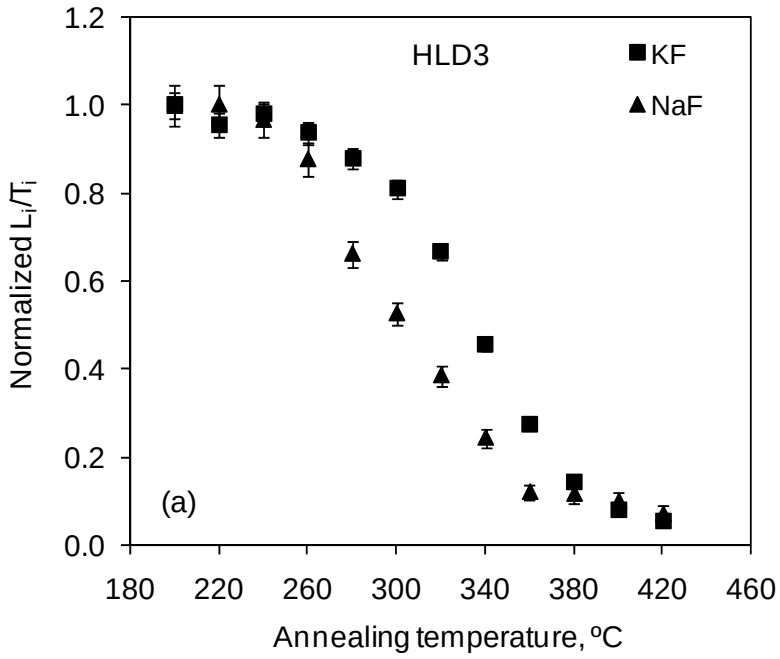
HLD3
KF
NaF
(a)
Normalized L_i/T_i
Annealing temperature, ºC
1.2
1.0
0.8
0.6
0.4
0.2
0.0
180
220
260
300
340
380
420
460

(b)

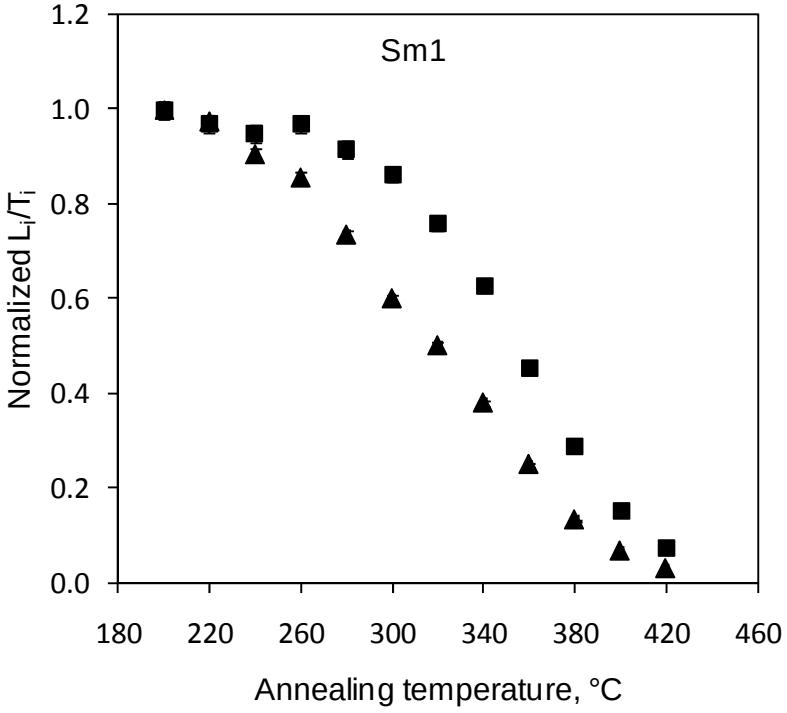
Sm1
Normalized L_i/T_i
Annealing temperature, °C
1.2
1.0
0.8
0.6
0.4
0.2
0.0
180
220
260
300
340
380
420
460

Figure 2

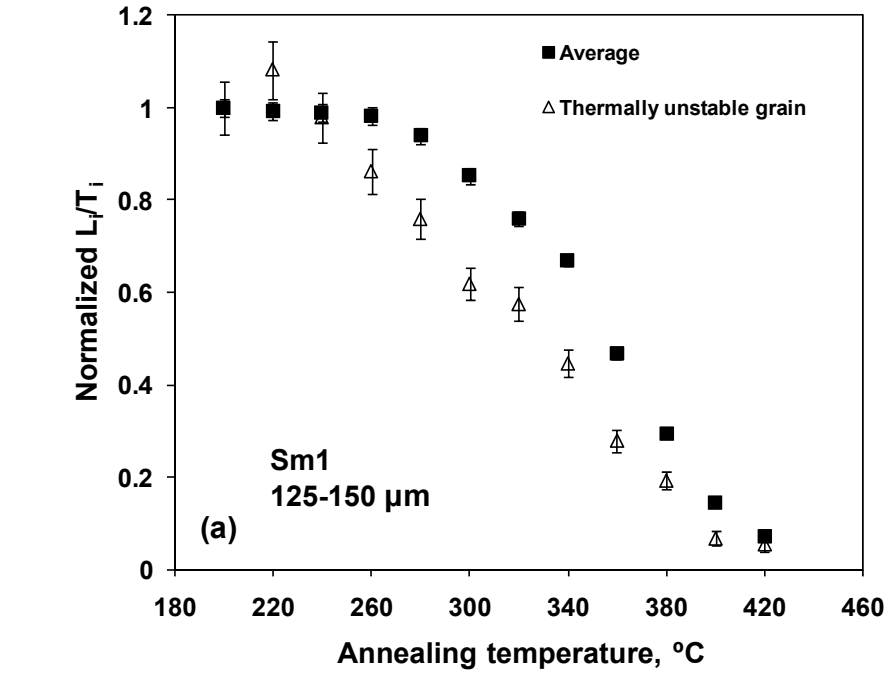
Average
Thermally unstable grain
Normalized L_i/T_i
Sm1
125-150 µm
(a)
Annealing temperature, °C

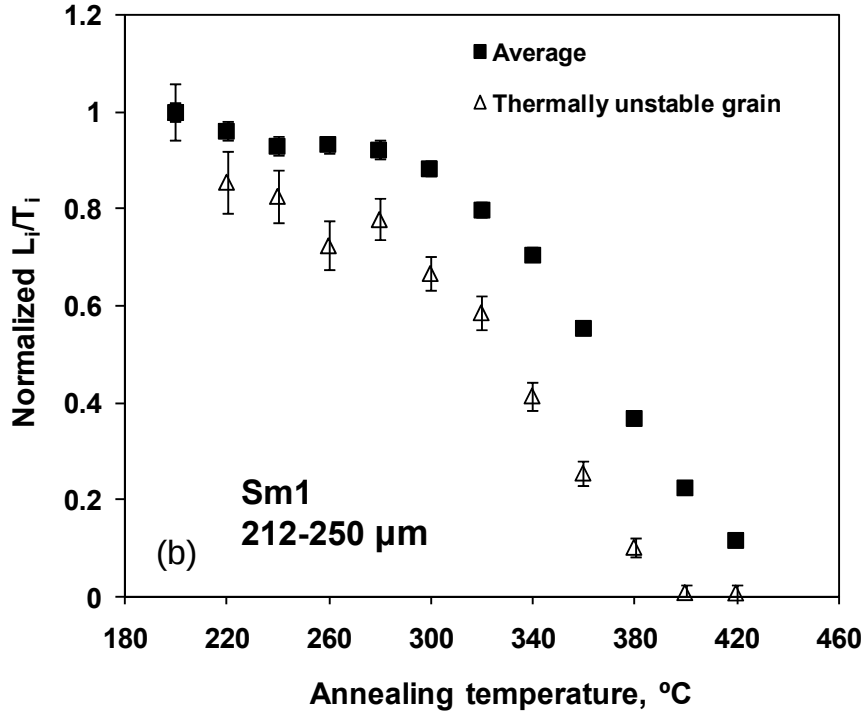
Average
Thermally unstable grain
Normalized L_i/T_i
Sm1
212-250 µm
(b)
Annealing temperature, °C

Figure 3

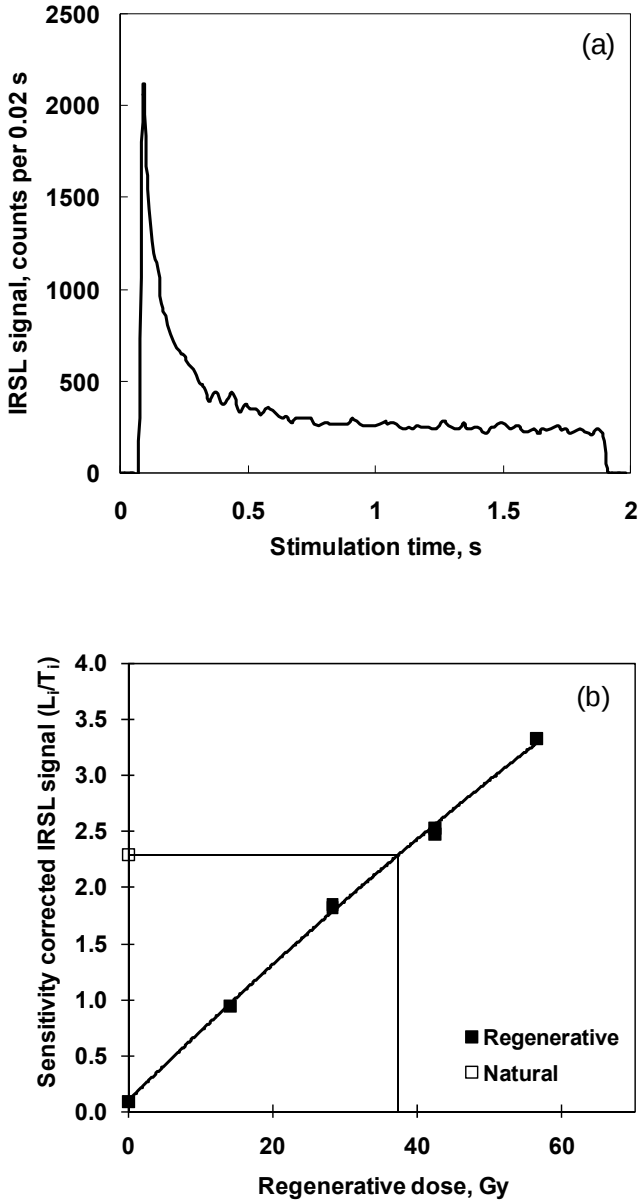
(a)
IRSL signal, counts per 0.02 s
2500
2000
1500
1000
500
0
0
0.5
1
1.5
2
Stimulation time, s
(b)
Sensitivity corrected IRSL signal (L_i/T_i)
4.0
3.5
3.0
2.5
2.0
1.5
1.0
0.5
0.0
0
20
40
60
Regenerative dose, Gy
Regenerative
Natural

Figure 4

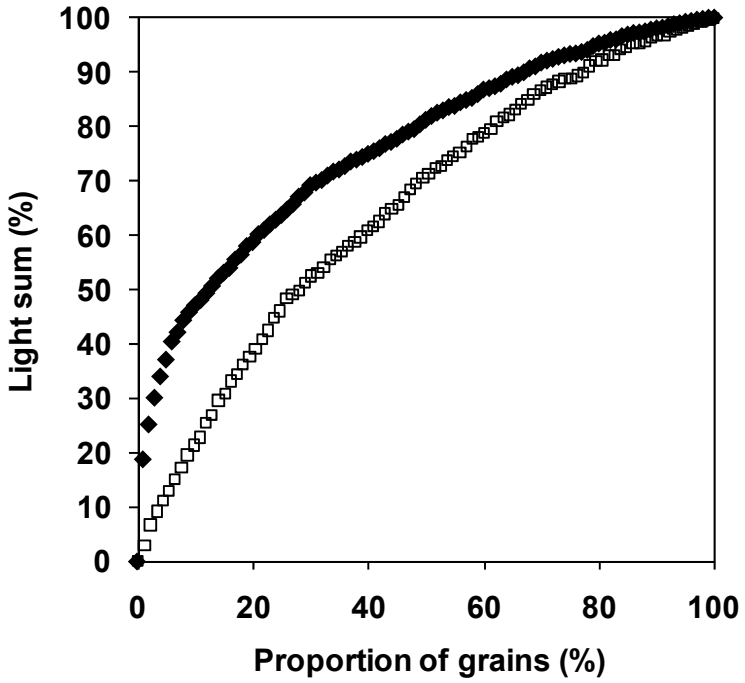
Light sum (%)
Proportion of grains (%)
0
10
20
30
40
50
60
70
80
90
100
0
20
40
60
80
100

Figure 5

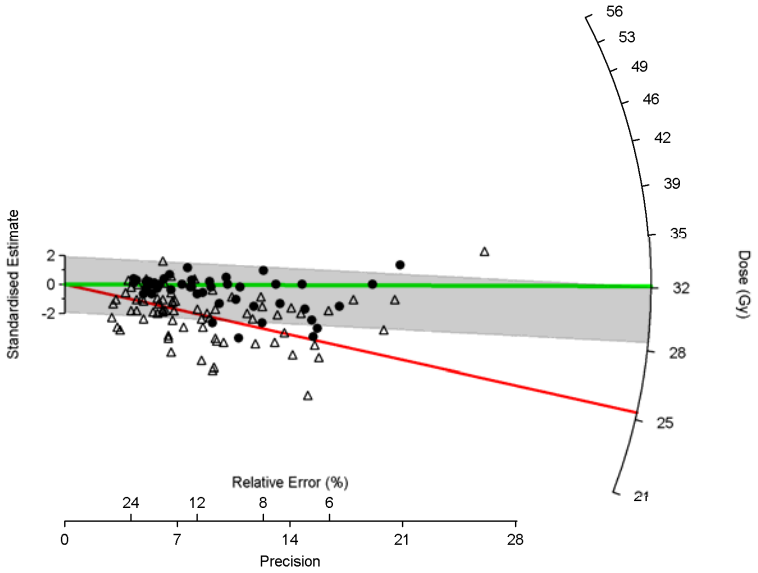
Standardised Estimate
2
0
-2
Relative Error (%)
24
12
8
6
0
7
14
21
28
Precision
56
53
49
46
42
39
35
32
28
25
21
Dose (Gy)

Figure 6

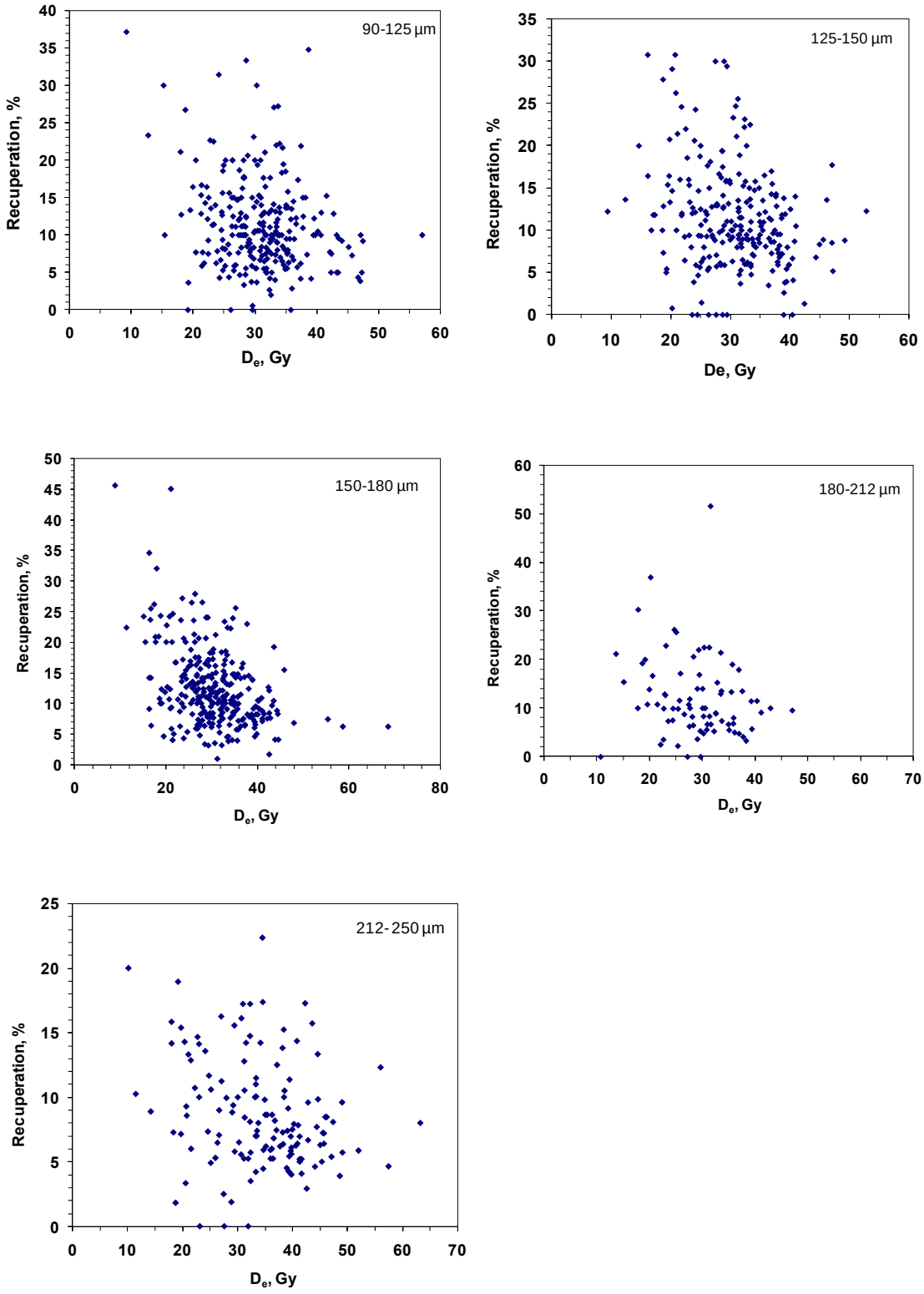
90-125 µm
Recuperation, %
De, Gy
125-150 µm
Recuperation, %
De, Gy
150-180 µm
Recuperation, %
De, Gy
180-212 µm
Recuperation, %
De, Gy
212- 250 µm
Recuperation, %
De, Gy

Figure 7

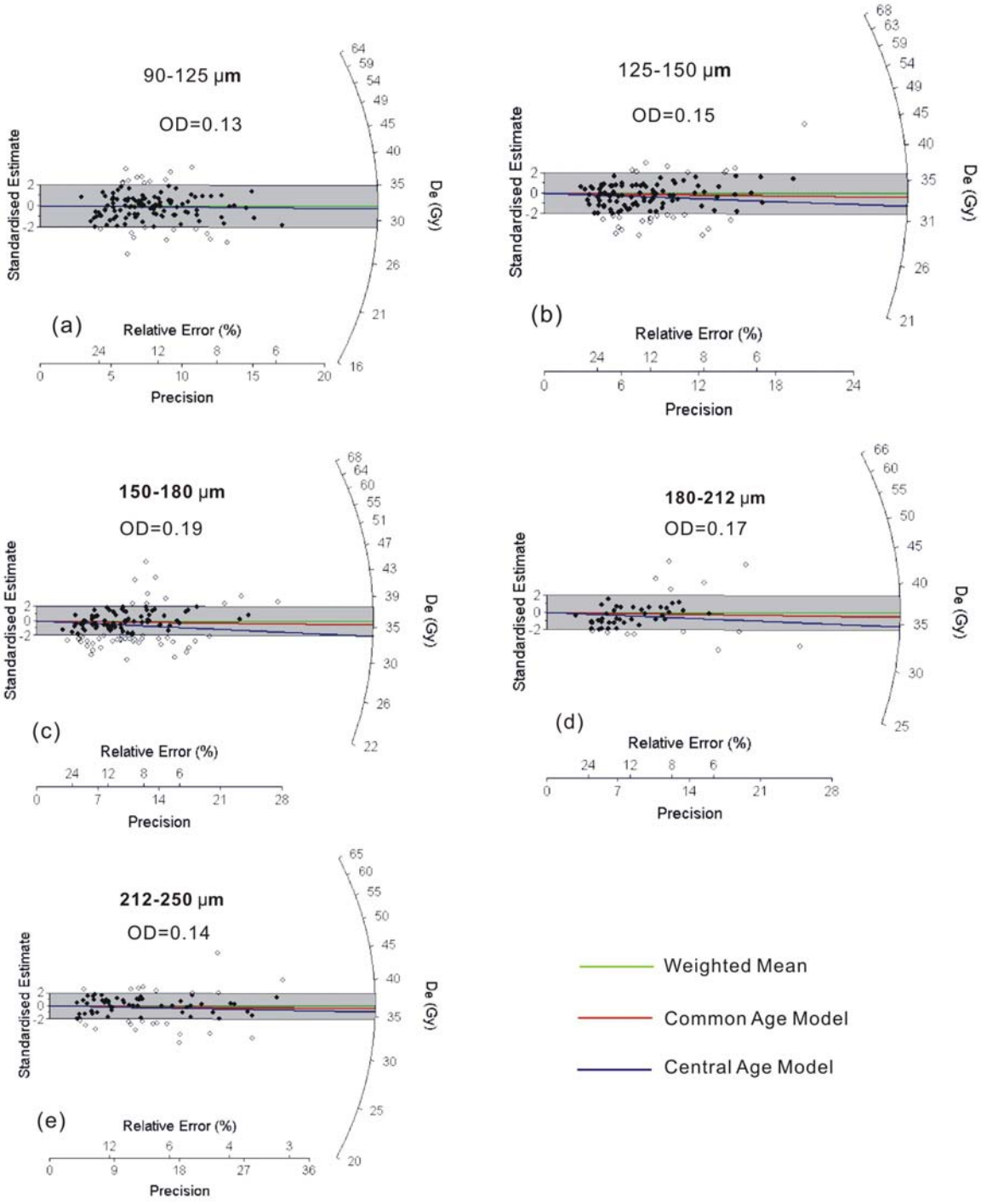
90-125 µm
OD=0.13
(a)
125-150 µm
OD=0.15
(b)
150-180 µm
OD=0.19
(c)
180-212 µm
OD=0.17
(d)
212-250 µm
OD=0.14
(e)
Standardised Estimate
De (Gy)
Relative Error (%)
Precision
Weighted Mean
Common Age Model
Central Age Model

Figure 8

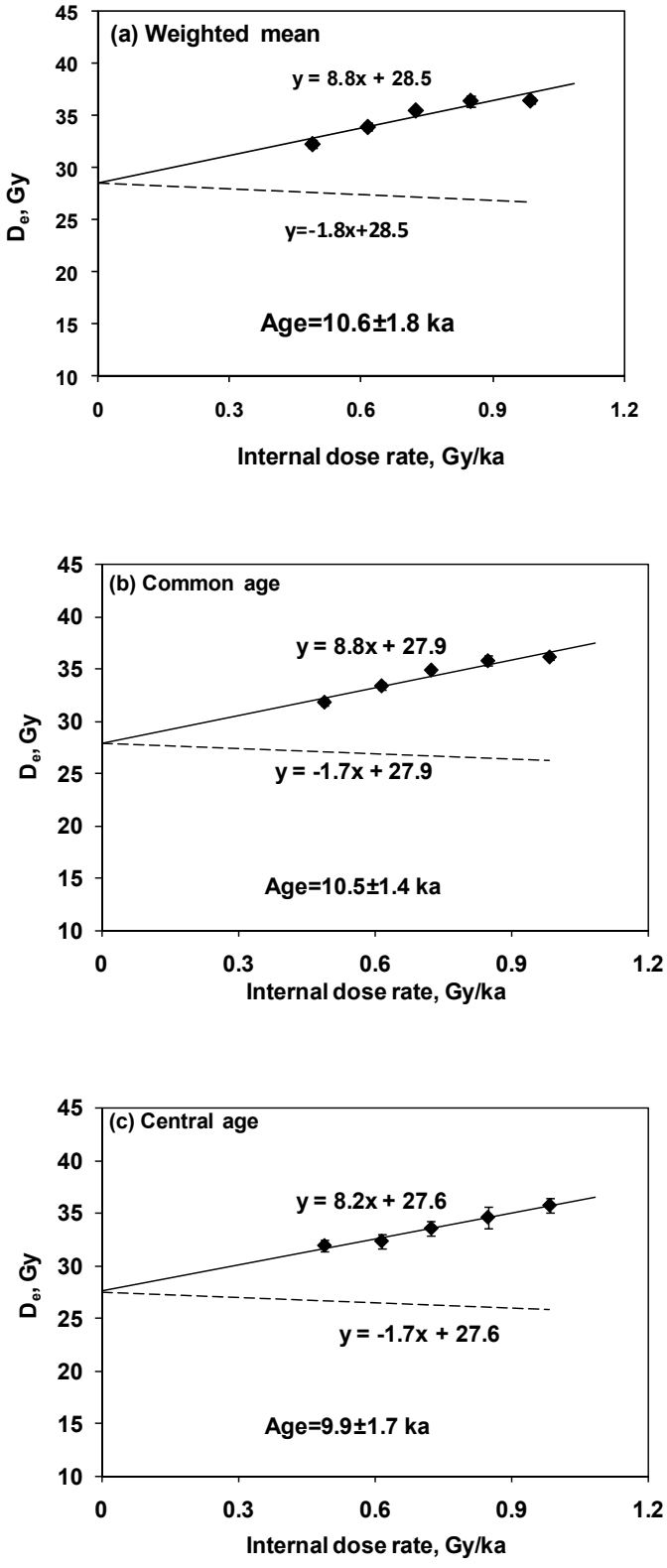
(a) Weighted mean
y = 8.8x + 28.5
y=-1.8x+28.5
Age=10.6±1.8 ka
(b) Common age
y = 8.8x + 27.9
y = -1.7x + 27.9
Age=10.5±1.4 ka
(c) Central age
y = 8.2x + 27.6
y = -1.7x + 27.6
Age=9.9±1.7 ka
De, Gy
Internal dose rate, Gy/ka
45
40
35
30
25
20
15
10
0
0.3
0.6
0.9
1.2

Figure 9